Stress-Induced Crystallization and Reinforcement in Filled Natural Rubbers: ^{2}H NMR Study

J. Rault,*,† J. Marchal,† P. Judeinstein,‡ and P. A. Albouy†

Physique des solides, Bat 510, Université Paris Sud, Orsay, 91405, France, and ICMMO, Bat 410, Université Paris Sud, Orsay, 91405, France

Received April 14, 2006; Revised Manuscript Received September 21, 2006

ABSTRACT: Stress-induced crystallization (SIC) and stress-induced melting (SIM) in pure and filled (carbon black, CB) natural rubbers are studied by mechanical analysis, X-ray scattering, and quadrupolar NMR as a function of temperature and filler content. These complementary techniques allow to measure the crystallinity and the local deformation of the amorphous chains during the mechanical cycle. The critical draw ratio for appearance (stretching) and disappearance (recovery) of the crystallinity are compared by these three techniques. It is shown by WAXS that CB particles act as nucleation centers of the SIC. By ^{2}H NMR one finds that during crystallization in both types of materials the remaining amorphous chains relax partially, as predicted by Flory. The amplification factors A_σ, A_χ, and A_{NMR} deduced from the stress crystallinity and NMR splitting measurements are compared. The amplification factors measured by WAXS (A_χ) and NMR (A_{NMR}) are of the same order and are not far from the Bueche prediction. The amplification factor A_σ deduced from the stress−strain curves verifies the classical empirical Guth and Gold relation. The relation $A_\sigma = 2.5A_{NMR}$ observed at low deformation (no SIC) indicates that the reinforcement in these filled rubbers has two causes of similar importance: the classical overstrain of the chains due to geometrical effect and the role of particles as new effective cross-links. When the samples (filled and unfilled) crystallize, a third reinforcement effect appears; the crystallites act also as giant cross-links, and the stress increases drastically with the macroscopic deformation (hardening).

1. Introduction

It is well-known that natural rubber (NR) and filled natural rubbers (F-NR) have excellent mechanical properties.[1−7] Since the discovery of the reinforcement of rubber by carbon blacks in 1904, filled rubbers are used to manufacture a wide range of materials. Solid particles (filler) can strongly improve the mechanical properties, tensile strength, tear resistance, hardness, and abrasion resistance. This effect has been the subject of an enormous amount of works, and there is still a debate about its microscopic origin. It is recognized that the polymer−solid surface interaction and the structure of the aggregates (morphology and size) play a major role. When strained, natural rubber crystallizes. Since the pioneer work of Flory[8] in 1947, various authors have studied the stress-induced crystallization (SIC) of pure vulcanized rubbers; references are found in different books.[1,9,11] However, the term "strain-induced crystallization" would be more appropriate because crystallization is due to the decrease of entropy of the strained chains and not to the increase of the stress. As reported by Gent[9−11] and by Thomas et al.,[12] the SIC effect in pure and filled NR would explain its excellent mechanical properties, in particular its resistance to crack propagation. Around an heterogeneity or at the crack tip of a flaw, the chains are much more extended than in the bulk; crystallization of such chains in pure and synthetic NR stops the propagation of the crack, and the material has then a high tensile strength.[13−15] Obviously the same process occurs in filled NR.[16] Flory in his book[17] (1953) noted that hardening in pure NR could be due to the formation of crystallites, these particles playing the role of filler. In other words, the exceptional properties of filled NR would be due to the presence of both types of solid particles, fillers, and crystallites. To understand the origin of the reinforcement, it is then necessary to separate the effects of these two types of solid particles. In crystallizable rubbers crystallinity depends on deformation and temperature. To estimate the relative influence of the two processes, it is essential to study the reinforcement of filled natural rubber as a function of the deformation and temperature. This is the aim of this work.

Numerous models (homogeneous and heterogeneous) have been proposed to apply the statistical theory of rubber elasticity to filled (noncrystallized) rubber; reviews on this subject have been given by Kraus,[18] Dannenberg,[19] and Göritz et al.[20−22] The main reason for the rise in stiffness and in tensile strength of filled rubbers is not well understood. Generally it is assumed that the deformations are homogeneous and are amplified locally by the presence of the particles. Also, another source of reinforcement would be due to the perturbation of the chain distributions through an excluded volume effect from the filler particles; the role of the interaction between the chains and the surface of the fillers has been clearly demonstrated. To understand the origin of the reinforcement, it is necessary to study the behavior of the chains near and far from the particles. In this work we are mainly interested in the behavior of the chains far from the particles. During deformation the orientations of these chains having a high mobility (∼80 °C above T_g) are followed by ^{2}H NMR. It is important to recall that the comparison of the local extension of the amorphous chains of filled and unfilled rubber permits to define a strain amplification factor; the value of this factor in fact depends on the property analyzed and therefore on the technique used.[16]

The central purpose of this work is to investigate the role of filler on the matrix deformation and on the stress reinforcement in NR filled with different concentration of carbon black. This paper is arranged as follows:

In section 2 we recall the various definitions and origins of the amplification factors and discuss the origin of the reinforcement of filled rubbers.

† Physique des solides, Bat 510.
‡ ICMMO, Bat 410.

10.1021/ma0608424 CCC: $33.50
Published on Web 10/28/2006

In section 3 we present the materials and detail the experimental conditions.

In section 4.1 we compare the SIC and SIM properties of filled NR with different carbon black (CB) concentrations. During deformation cycles, stress−strain curves, and crystallinity curves at different temperatures are recorded simultaneously; the critical draw ratios for the onset of crystallization (stress hardening) and for melting (stress softening) are then determined. We show that CB particles must be considered as nucleation centers of the crystallites during SIC. As in pure NR the mechanical hysteresis is found to be proportional to the maximum crystallinity appearing at the maximum draw ratio during the cycle. It is shown that the strain amplification factors deduced from mechanical and crystallinity measurements are very different.

In section 4.2 we compare the extension of the amorphous chains in NR and F-NR, during drawing before crystallization, during stress hardening process (crystallization), and then during recovery (melting). The extension of the amorphous chains during SIC and SIM is measured by quadrupolar NMR; the samples contain small amounts of deuterated probes. From the comparison of filled and unfilled samples we deduce the true strain amplification factor (SA) $A_\epsilon = A_{NMR}$ (eq 1a), a function of the filler content and of the crystallinity. This SA factor is compared to the other factors A_σ and A_χ deduced from mechanical and crystallinity curves. The relation $A_\sigma > A_{NMR}$ at low deformation permits to estimate the role of the filler as equivalent cross-links.

2. Amplification Factors

In composite rubber matrix containing undeformable filler particles, one expects an effectively increased strain within the soft matrix. (This will not be true during SIC; it will be shown that crystallization produces a decrease of the chain deformation.) The strain amplification factor A_ϵ is defined by the relation

$$A_\epsilon = \frac{\epsilon_l}{\epsilon} = \frac{\lambda_l - 1}{\lambda - 1} \tag{1a}$$

where ϵ and ϵ_l are the macroscopic and local strains in the filled rubber and λ and λ_l are the corresponding draw ratios. This amplification factor will be called the true strain amplification (TSA) factor. The local extension of the chains in rubbers has been measured by polarized infrared spectroscopy,[5,23] quadrupolar NMR,[24−36] and small-angle neutron scattering.[37−39]

On simple geometrical consideration the relation between the strains ϵ and ϵ_l in the noncrystallizable matrix can be calculated. For a simple arrangement of particles, the local strain in the rubber phase can be put on the form

$$\epsilon_l/\epsilon = (1 - C^x)^{-1} \tag{1b}$$

C is the volume fraction of the filler ($C < 0.3$ in most studies), and x is an exponent which depends on the structure of the periodical arrangement of the particles in the rubber matrix. In a 3-dimensional arrangement of monodisperse spherical particles, $x = 1/3$, this is the Bueche expression.[40,41] For 1-dimensional arrangement of rigid and soft lamellae of constant thickness, $x = 1$. In filled rubber it is well-known that the arrangement of the particles is complex, and aggregates with a large size distribution are observed. Also, the arrangement of the particles can be modified during deformation. Hence, the prediction of the exponent x in these real materials is not straightforward. Obviously, in any case, this relation is valid only when the rubber has not crystallized. Generally the volume fraction is low, $C < 0.3$; the strain amplification factor A_ϵ deduced from the above expression ($x = 1/3$) is then

$$A_\epsilon \sim (1 + 2.95C); \quad C < 0.3 \tag{1c}$$

A similar expression has been proposed by Botti et al.[42] Several authors assume that the volume concentration in eq 1 is in fact an effective concentration which must take into account the polymer layer in interaction with the fillers surface. Guth and Gold[43] defined a different amplification factor A_E as the ratio of the moduli of filled (E) and unfilled (E_0) rubbers. They suggested that this modulus amplification factor due to hydrodynamic effect has the form

$$A_E = \frac{E}{E_0} = 1 + aC + bC^2 \tag{2}$$

where a and b are the constants of the Einstein viscosity equation ($a = 2.5$, $b = 14$) of a system of rigid spheres in interaction in a fluid. Various theories (see ref 3) based on the elasticity of composite systems lead to a similar relation, but agreement with the experiments is somewhat less satisfactory. Mullins and Tobin[44] interpreted A_E as being the strain amplification factor; in fact, the rubber is a nonlinearly elastic material, and therefore in the above relation the modulus cannot be replaced by the strain (at constant stress). It must be noted that the similarity between the concentration dependence of A_ϵ and A_E is fortuitous; the definitions of these factors rely on static (eq 1c) and dynamic arguments (eq 2). Equation 2 is well verified in noncrystallizing rubbers; this is the reason why it seems relevant to conclude that the reinforcement of rubber by filler is analogous to the increase of viscosity in fluid containing rigid particle. In fact, Kraus[1] concluded that "the interpretation of eq 2 as a strain amplification relation and its extension to large strains are based on intuitive reasoning rather than on rigorous proof". Flory in his book noted that during vulcanization extensive bonding occurs at the filler surface. These bonds so formed constitute additional points of constraint, and a layer of higher modulus of elasticity of thickness ~50 Å (chain length) around each particle is formed. This author concluded that "it may be legitimate to consider that the matrix as a whole is stiffened by the formation of bonds between the rubber chains and the filler surface. Under these conditions eq 2 cannot be applied unambiguously." As remarked by Mark et al.[5] "a filled rubber may be regarded as a polymer network containing giant network cross-link (GNC)". The effect of cross-linking of rubbers by fillers has been reviewed by Rajeev and De.[45] Castaing et al.[46] demonstrated clearly that long PDMS chains grafted on silica particles lead to a reinforced material even when there is no chemical cross-linking between the chains.

The effect of reinforcement in natural rubber is a more complicate phenomenon because stress-induced crystallization occurs above a critical draw ratio, and this leads to an other (intrinsic) reinforcement effect. As noted above, the excellent mechanical properties of natural rubber are due to stress-induced crystallization. At high strain above a critical draw ratio hardening is observed. This effect leads Flory to conclude that crystallites (as the fillers) would play the role of new cross-link in crystallizable rubbers.

The aim of this paper is to estimate the effects of the equivalent GNC (effective cross-link) due to filler and crystallites on the on the local draw ratio λ_l and on the density of new effective cross-links d_{GNC} and d_{cryst} due to the filler and to the crystallites. For this purpose we compare the strain amplification factors A_X (A_σ, A_χ, A_{NMR}) deduced from the stress $\sigma(\lambda)$,

crystallinity $\chi(\lambda)$, and NMR splitting curves $\Delta\nu(\lambda)$:

$$A_X = \epsilon_f/\epsilon \tag{3}$$

where $\epsilon_f = 1 - \lambda_{F-NR}$ and $\epsilon = 1 - \lambda_{NR}$ are the macroscopic strains of the filled and unfilled rubbers which lead to the same property X. These strain amplification factors determined by mechanical measurements (A_σ), crystallinity measurements (A_χ), and NMR (A_{NMR}) are compared at low and high deformations. It is emphasized that the influence of the stress-induced crystallization on these amplification factors in filled NR has never been studied in detail.

3. Experiments

3.1. Materials. The materials natural rubbers (NR) and filled natural rubbers (F-NR), provided by Michelin Co., have been obtained by sulfur vulcanization (1.2 g of sulfur per 100 g of rubber). All materials contain the same amount of ingredients; per hundred gram of rubber (phr), stearic acid 2 g, zinc oxide 5 g, antioxidant 1 g, and accelerator 1.2 g; the materials without filler have been previously studied in refs 14−16. Three series of F-NR (with NR containing 1.2 g of sulfur) have been studied; they contain 20, 40, and 50 g of carbon black (N375) per hundred grams of rubber (phr). The concentration of the fillers is 13, 26, and 33% in weight (8, 16, and 20% in volume); the densities of amorphous NR and CB are 0.92 and 1.60 g/cm^3. The cross-linking density d_{cl} of the unfilled natural rubber deduced from modulus and swelling measurements is (5.7−6.0) × 10^{-5} mol/cm^3. The number of monomers between cross-links is $N_C = \rho/M_0 d_{cl} = 238$; $M_0 = 68$ g/mol is the molecular weight of the monomer, and $\rho = 0.92$ g/cm^3 is the density of natural rubber NR. As noted below, the molecular weight $M_c^* = N_C M_0$ between cross-links is in fact an effective mass which depends on the density of entanglements, $d_e \sim 1/M_e$, trapped in the network. According to Elias,[47] the mass of the chains between entanglements in a non-cross-linked NR is $M_e = 20\,100$. The mechanical and crystallinity properties of the NR samples with the same composition have been analyzed in refs 15 and 16 (called sample II in these references). All samples have dumbbell shape with the same dimensions; length 30 mm, section 1 × 3 mm^2.

3.2. Instrument and Procedure. The experimental setup for simultaneous mechanical and X-ray measurements have been described in refs 14 and 16. For measuring the crystallinity only the (200) NR reflection was recorded with a linear counter. WAXS intensities of the (200) reflection and of the amorphous halo were corrected taking into account the change of thickness during deformation and the concentration of CB. The absorption coefficient and the thickness of the sample during experiments were measured by a photodiode along the central X-ray beam (with and without the sample). The stress−strain curves are obtained at 2 mm/min ($\epsilon' = 0.001$ s^{-1}). The X-ray acquisition time is 60 s; for $\lambda = 7$ the time of a cycle is 171 min. From the WAXS spectrum and from the transmitted central beam (giving the thickness h) one calculates the intensity of the amorphous halo $I_a(s)$ (at constant thickness), and the total crystalline intensity I_c of the sample which would have the same constant thickness. As noted above, only the intensities in the XOY plane of the CCD camera are taken into account. The index of crystallinity $\chi = I_c/I_a \times 100$ is then calculated. This procedure is somewhat different from Mitchell's one.[48]

For ^{2}H NMR measurements, the samples were swollen with 1−2% of deuterated dodecane. A stretching device permits to draw the sample in the NMR tube (diameter 10 mm). The stretching direction of the sample is parallel to the magnetic field. The NMR spectra were recorded on a Bruker AM 360 spectrometer (H-2 frequency 55.3 MHz), and the spectral width was limited to 10 000 Hz. Previous studies have shown that the NMR splitting is independent of the concentration ($C < 4\%$). 2000 transients were acquired for each spectrum (acquisition time is 10 min). To relax the samples after the next stretching, 5 min delay was used between each measurement. The time for doing a complete stretching−relaxation cycle (a series of 15 NMR spectra) is about 225 min. In conclusion, the durations of mechanical and NMR cycles are comparable. In all the experiments the draw ratio λ was deduced from the distance of ink marks on the samples.

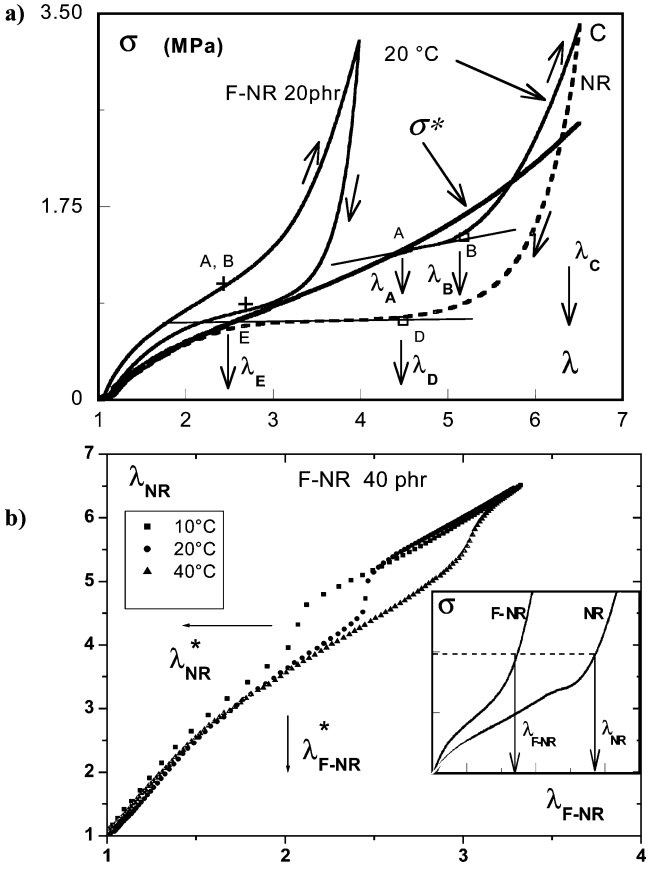

Figure 1. (a) Mechanical cycles of NR and F-NR 20 phr at $T_1 = 20$ °C, speed 1 mm/min, initial length *30* mm. The stretching curve σ^* (heavy line) is the experimental stretching curve of the NR sample at $T_2 = 72$ °C (without stress-induced crystallization) taking into account the temperature correction T_1/T_2 (see text). This would be the hypothetical stress−strain curve of the sample at $T_1 = 20$ °C which would not crystallize. The critical draw ratios of appearance, λ_A, and disappearance, λ_E, of the crystallinity are indicated. (b) Method to measure the strain amplification factor A_σ of F-NR 40 phr at three temperatures. Correspondence between the draw ratios λ_{NR} and λ_{F-NR} which lead to the same value of the stress of the filled and unfilled samples; see text. The stress−strain curves (stretching) of the NR and F-NR sample are plotted in the inset. At low deformation A_σ, the slope of the curve $\lambda_{NR}(\lambda_{F-NR})$ is constant. The jump of the curves is due to SIC; the values of λ^*_{NR} and λ^*_{F-NR}, arrows for sample at 10 °C, correspond to the characteristic ratio λ_A at the onset of crystallization.

The basic concepts of ^{2}H NMR in anisotropic fluids are given in refs 49 and 50. A large amount of work (see references in the review paper of Deloche and Sotta[33]) has shown that the local segmental order in stretched elastomers can be monitored accurately by the splitting $\Delta\nu$ of lines in the ^{2}H NMR spectra, the deuterated probes being solvent molecules or the chains itself. In a previous work,[51] we have shown that deuterated alkanes, C_nD_{2n+2}, sufficiently long ($n > 8$) and in low concentration ($C < 4\%$) are good candidates to follow the orientation of the NR matrix during stretching, recovery, and stress relaxation at any temperature between −10 and 100 °C.

4. Results and Discussion

4.1. Mechanical and Crystallinity Properties. *4.1.1. Mechanical Cycles. (a) Determination of the Characteristic Draw Ratios from Mechanical Cycles.* SIC and SIM during mechanical cycles in pure NR of different cross-link density have been studied previously.[15,16,51−56] Figures 1 and 2 give examples of

mechanical cycles of NR and F-NR sample at various temperatures. As for nonfilled NR[52,53] we define the different characteristic draw ratios: λ_A and λ_B during stretching; λ_D and λ_E during recovery. λ_C corresponds to the maximum drawing during the cycle. λ_A and λ_B correspond to the beginning of crystallization and the end of melting, and λ_D corresponds to the beginning of the recovery plateau. The six different domains can be easily distinguished in Figure 1a: OA is the Mooney and Rivlin (MR) domain; AB is the (inclined) stress plateau; BC and CD the hardening domains due to SIC and SIM; DE is the recovery stress plateau; EO is the small deformation domain where elasticity theories applies. As reported by other authors, the main effect of fillers is to displace the mechanical cycle toward smaller elongation (amplification effect); some differences must be noted. In F-NR (a) the (inclined) plateau AB during stretching is not observed, and (b) the stretching and the recovery curves do not merge exactly. This is due to the creep effect.

This will impede an exact determination of the critical draw ratio by the mechanical measurements. From the similar form of the hardening domain (and its disappearance at high temperature) we can only suggest that crystallization and melting appear at the inflection points marked (+) in Figure 1a on the stretching and recovery curves. This will be confirmed by WAXS.

In Figure 1a we have plotted the corrected stress−strain curve $\sigma^*_{T_1} = \sigma_{T_2}(T_1/T_2)$ of unfilled NR at $T_1 = 20$ °C deduced from the experimental curve at $T_2 = 72$ °C; the temperature dependence of stress of noncrystallizing rubbers verifies the rubber elasticity theory, $\sigma \sim T$. The experimental curve at 72 °C does not present any hardening effect, and no crystallinity can be detected by WAXS up to $\lambda = 6$. The small curvature of the $\sigma_{T_2}(\lambda)$and $\sigma^*_{T_1}$ curves near $\lambda = 4.5$ would be due to the finite extensibility of the chains at high elongation; this reinforcement effect in NR is weak compared to the effect of SIC and will not be analyzed here. $\sigma^*_{T_1}(\lambda)$ is the curve of the "hypothetical" sample at $T_1 = 20$ °C, which would not crystallize. One verifies that this curve merges with the experimental curve only at low deformation when there is no SIC. In the figure we have drawn the tangents to the stress−strain curve $\sigma_{T_1}(\lambda)$ of the pure NR at the inflection points on the two (inclined) plateau AB and DE. The intersections of these tangents with the corrected curve $\sigma^*_{T_1}$ define the points A and E. We have shown that in pure NR the critical draw ratios λ_A and λ_E corresponding to SIC and SIM are deduced with the same accuracy from the stress $\sigma(\lambda)$ and crystallinity $\chi(\lambda)$ curves.[53] A similar procedure can be employed to determine the critical draw ratio λ_A in F-NR.

(*b) Determination of the Amplification Factor* A_σ. In Figure 1a we compare the behavior of the F-NR 20 phr with the unfilled sample drawn at $T_0 = 22$ °C up to $\lambda_{NR} = 6.4$ and $\lambda_{F-NR} = 4$; the maximum stress during the cycles is the same. One can verify that the cycles cannot be superimposed by the simple orthogonal transformation $1 - \lambda_{NR} \Rightarrow A_\sigma(1 - \lambda_{F-NR})$. In Figure 1b we have plotted for the 40 phr sample the correspondence between the draw ratios λ_{NR} and λ_{F-NR} which leads to the same stress value during stretching. This procedure was first used in ref 16 to calculate the amplification factor A_σ of F-NR samples. In the inset of the figure the stress−strain curves (stretching) of the two samples are schematized, an arbitrarily number n of stress values $n\Delta\sigma_0$ are chosen, the corresponding values (λ_{NR}, λ_{F-NR}) are recorded, and then the curve $\lambda_{NR}(\lambda_{F-NR})$ is drawn. A_σ, the slope of the vector linking the origin (1,1) and the point (λ_{NR},λ_{F-NR}) on the corresponding curve, is dependent on the macroscopic deformation λ_{F-NR}. For the three temperatures, 10, 20, and 40 °C two regimes separated by a crossover at λ^*_{NR} and λ^*_{F-NR} are observed (arrows in the figure for the sample at 10 °C). It will be shown below that the values λ^* correspond to the onset of crystallization λ_A in both types of NR. All filled samples present similar behavior. At low deformation the material is not crystallized, and λ_{NR} varies linearly with λ_{F-NR}; in that case the amplification factor A_σ is the slope of the curve $\lambda_{NR}(\lambda_{F-NR})$. From this curve we conclude that the amplification factor A_σ is constant at low deformation (independent of the temperature) and then varies at high deformation, when stress-induced crystallization occurs. It is important to remark that the departure from the linearity, λ_{NR} vs λ_{F-NR}, occurs somewhat before the crossover λ^*_{NR}; this clearly indicates that simple arguments leading to eq 1 cannot explain the observed behavior of filled NR at high strain, above $\lambda = 1.6$.

(c) Effect of Filler on the Elastic Modulus at Low Deformation. In the domain between $1 < \lambda < \lambda_A$, before the hardening domain, the nominal stress σ of NR and F-NR follows the semiempirical Mooney−Rivlin (MR) relationship[1−3]

$$\sigma = E_0/3(\lambda - \lambda^{-2})(C_1 + C_2/\lambda) \qquad \lambda < 4 \tag{4a}$$

for most NR studied in the literature; the chains between cross-links are rather long so the effect of the limiting extensibility of the chains is seen above $\lambda = 5$, and the hardening effect observed for $\lambda > \lambda_A$ is due to the crystallization. At small and large deformation, the above MR relation gives

$$\sigma \sim E_0(\lambda - 1) \qquad 1 < \lambda < 2 \tag{4b}$$

$$\sigma \sim d_{cl}\lambda \qquad 2 < \lambda < 4 \tag{4c}$$

where d_{cl} is the density of cross-links $d_{cl} = \rho/M_c$ (the chains linking two cross-links have N_c monomers of molecular weight M_0 ($M_c = N_cM_0$). C_1 and C_2 are the MR constants. The modulus $E_0 = F\rho RT/3M_c \sim d_{cl}$ is deduced from the classical rubber elasticity theory, and the front factor F depends on the choice of the molecular model of the network chain[5,17] (affine or phantom network, etc.). Here we are only interested in the effect of density of "effective" cross-links (due to sulfur bridge, entanglements, fillers), and then for simplicity reasons all the prefactors in eqs 4b and 4c are dropped.

In pure NR it is well-known that the deformation is affine; the macroscopic and local deformation are equal, and the nominal stress is proportional to the entropic term ($\lambda - \lambda^{-2}$). In filled rubber the deformation is not affine. If the above relation is applied, λ being the macroscopic draw ratio, then one finds that the modulus increases with the concentration of filler according to the Guth and Gold relation (eq 2). In fact, if one assumes that the chains in filled and unfilled NR form the same type of network (between fillers), the macroscopic draw ratio, λ, in the above equation must be replaced by the local one, $\lambda_l = 1 + A_\epsilon(\lambda - 1)$. Then the main question concerning the reinforcement at low strain is the following: Does eq 4 apply for the filled rubber (noncrystallizing) if the macroscopic strain is replaced by the local strain $\epsilon_l = A_\epsilon\epsilon$ and if the density of cross-links ($d_{cl} \sim 1/M_c$) remains constant?

In unfilled rubber the density of cross-links is deduced from modulus and swelling experiments. Several authors in fact pointed out that the density of cross-links d_{cl} is in fact an effective density which must take into account the presence of entanglements, which are trapped in the network and act also as new cross-links. Therefore, in eq 4 d_{cl} must replaced by the effective density d^*_{cl}, the sum of the cross-links (d_{cl}), and

entanglements ($d_e \sim 1/M_e$) densities:

$$d_{cl}^* = d_{cl} + d_e \sim \frac{1}{M_c^*} = \frac{1}{M_c} + \frac{1}{M_e} \quad (5a)$$

Dubault et al.[26] and Simon et al.[29,30] have verified this relation in PDMS and SBR networks by quadrupolar NMR. Simon et al.[57] found a good agreement between M_c values in *cis*-polybutadiene deduced from stress−strain measurements and by ^{1}H and ^{2}H NMR transversal relaxation methods.

In a similar manner, if any filler particle (and/or crystallites) is equivalent to a certain amount of sulfur cross-links as suggested by Flory, then we must write

$$d_{cl}^* = d_{cl} + d_e + d_{GNC} \sim \frac{1}{M_c^*} = \frac{1}{M_c} + \frac{1}{M_e} + \frac{1}{M_{GNC}} \quad (5b)$$

M_{GNC} is a phenomenological parameter which describes the cross-linking effect of the fillers.

Chemical cross-links, entanglements, and chains adsorption on the filler contribute to the total network density, called hereafter effective density. For simplicity reasons, we assume that M_c and M_e are not dependent on the filler concentration. It is relevant to assume that the effective density $d_{GNC} \sim \rho/M_{GNC}$ of GNC is proportional to the filler content (more exactly to the total surface area of the fillers). In that case the local modulus $G_m \sim d_{cl}^*$ varies linearly with C. This modulus must not be confused with the macroscopic modulus E. One must note the difference between fillers and crystallites; d_{GNC} does not depend on λ in filled rubber at low deformation (no SIC) if the interaction filler chains do not change during deformation. In pure and filled rubbers when SIC occurs, we expect that d_{GNC} increases with λ; the number of crystallites (GNC) per unit volume increasing linearly with λ.

The above relation is not totally new; Maier and Göritz[58] used a similar relation for interpreting the Payne effect; in their model the density of effective cross-links due to the unstable bonds between chains and filler is dependent on the strain amplitude. Berriot et al.[59] also used the above relation to interpret their ^{1}H NMR relaxation results on polyacrylate matrix filled with silica particles; the additional constraint density ($d_{GNC} \sim 1/M_{GCN}$) was found to increase proportionally to the total surface area of the filler introduced in the matrix. Litvinov et al. used this relation to explain the reinforcement mechanism of filled EPDM.[34]

The strain amplification deduced from the stress−strain curves (and from other properties) would have two origins: the amplification of the local strain due to geometrical considerations and the amplification of the local modulus due to the new cross-links formed by the crystallites and the fillers.

(d) Effect of Filler in the Hardening Domain. At high strain, above the critical draw ratio λ_A, hardening is observed in both types of rubbers, and eq 4a is no longer valid. The stress increases drastically with the macroscopic draw ratio, λ, according to the scaling form[51−53]

$$\sigma \sim \sigma(\lambda_A) + k\lambda(\lambda - \lambda_A); \quad \lambda > \lambda_A \quad (6)$$

where k is a constant. The second term which describes the hardening is due to the crystallization of the rubber.[5] In noncrystallizable rubber (for example SBR) hardening is also observed; this well-known effect is due to the finite extensibility of the chains. Flory in his book[17] suggested also that small crystallites in cross-linked crystallizable elastomers could be visualized as new type of cross-link, which would be the cause of the hardening observed in NR drawn at high extension. This

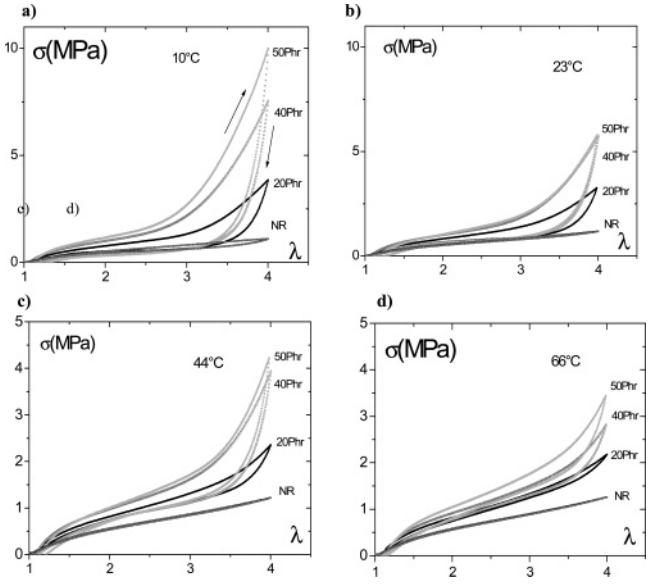

Figure 2. Stress−strain curves (cycles) of filled and pure NR samples at various temperatures (10, 23, 44, 66 °C). Strain rate 0.033 s^{-1}, maximum draw ratio $\lambda_C = 4$. At low deformation ($\lambda < 4$) natural rubber does not crystallize. The upturn of the stress for filled rubbers is due to the stress-induced crystallization.

effect in NR has been discussed recently;[51] in the hardening domain the local draw ratio λ_l of the amorphous chains (measured by NMR) is constant ($\lambda_l = \lambda_A$), and the increase of σ with the macroscopic deformation λ is due to the increase of the crystallites density d_{cryst} and not to the limiting extensibility of the amorphous chains. Each new crystallite formed acts as a new cross-link or a series of cross-links which reinforce the material. The process of crystallization is described in Figure 13 of ref 53. Obviously in filled natural rubbers the same SIC effect occurs and locally leads to the same process of reinforcement. Then to understand the origin of reinforcement, it is necessary to separate the effects of crystallites and those of fillers on the local deformation of the amorphous chains. These two types of rigid particles would have a common characteristic: they can be considered as giant network cross-links (GNC).

4.1.2. Crystallinity Cycles. (a) Critical Draw Ratios λ_A and λ_E. In Figure 3 we present crystallinity curves of the different samples during the mechanical cycles at four temperatures. By WAXS analysis one observes that the melting of the crystallites is progressive between λ_C and λ_E; it has been shown previously[52,53] that during this process the volume and dimensions of the crystallites do not change, while their number decreases linearly with T. Both critical draw ratios increases with T. As the crystallinity varies linearly with the deformation, by WAXS the critical draw ratios λ_A and λ_E can be determined with accuracy ($\Delta\lambda < 0.2$); this was not the case by mechanical measurements.

In Figure 4 the stress−strain and crystallinity−strain curves of two F-NR samples, 20 and 50 phr, at room temperature are given for different maximum draw ratio λ_C. All these results indicate clearly that the reinforcement above the critical draw ratio λ_A (hardening) is due to the stress-induced crystallization and not to the limited extensibility of the chains. In F-NR samples it is then necessary to separate the reinforcement effects above and below λ_A (and λ_E) and to know the dependence of these characteristic draw ratios for SIC and SIM with the filler content.

In Figure 5 we have reported for a same macroscopic draw ratio, $\lambda = 4$, the engineering stress, σ, of all rubbers as a function

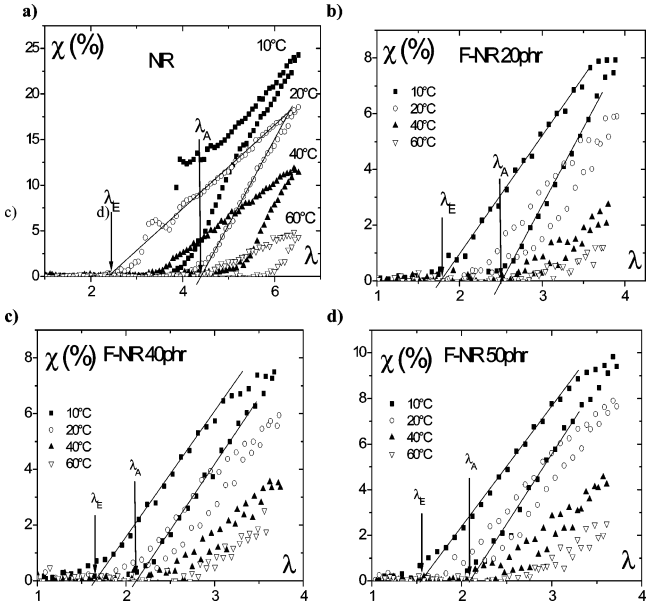

Figure 3. Crystallinity χ of filled and pure NR samples during mechanical cycles at various temperatures. Definition of the critical draw ratios λ_A and λ_E corresponding to the beginning of crystallization and to the end of melting. Lines for $T = 20$ °C are guides for the eyes.

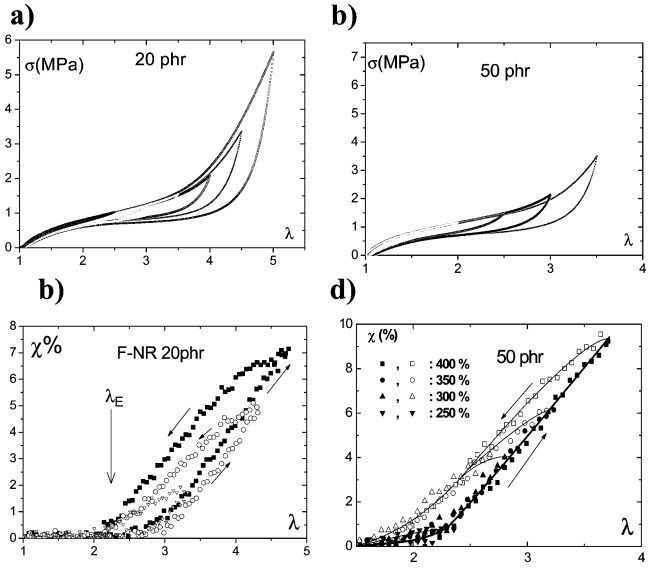

Figure 4. Mechanical and crystallinity cycles of F-NR 20 and 50 phr for different maximum extension λ_C. For more clarity all the crystallinity points are not given. The mechanical hysteresis is proportional to the maximum crystallinity obtained at the maximum draw ratio of the cycle.

of the phr content of carbon black and for different temperatures. At 60 °C, the F-NR and NR samples have not crystallized (no SIC at $\lambda = 4$). Compared to the NR sample, the stress of the 50 phr sample has been amplified by a factor 2. At 10 °C the crystallinity are 0 % (NR) and 10% (F-NR), and the stress of the F-NR sample has been amplified by a factor 10. This example clearly shows the importance of reinforcement due to SIC.

We have determined the variations of λ_A and λ_E with the filler content and the temperature; the estimated error is about $\Delta\lambda \sim 0.2$. These characteristic ratios are reported in Figure 6a as a function of temperature for NR and F-NR (50 phr); for more clarity the results for the other samples are not given. The difference $\Delta\lambda = \lambda_A - \lambda_E$ for all samples is plotted as a function of T in Figure 6b. From these two figures we conclude:

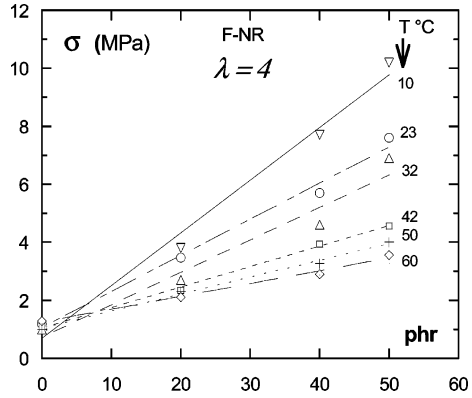

Figure 5. Engineering stress of filled NR strained at $\lambda = 4$ as a function of phr content and temperature. At 60 °C the materials are not crystallized. At constant phr reinforcement is due to the stress-induced crystallization. Lines are linear regressions.

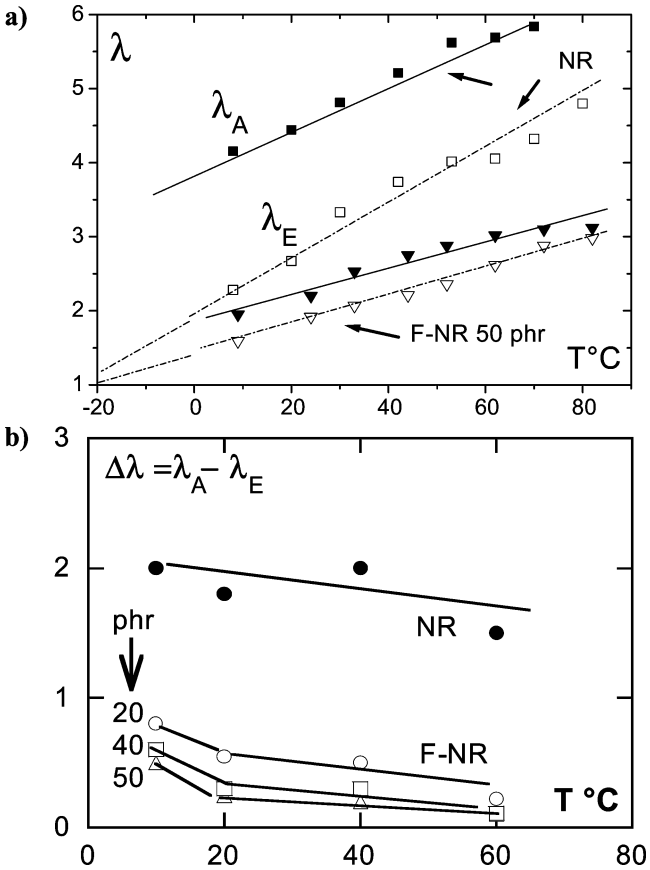

Figure 6. (a) Critical draw ratio λ_A and λ_E for onset of crystallization and for complete melting in NR and filled NR *50* phr as a function of temperature. Lines are linear regression. (b) Difference $\lambda_A - \lambda_E$ as a function of temperature for the NR and F-NR samples. Lines are guides for the eyes.

(1) The draw ratio λ_E of NR and F-NR at the end of melting verifies the linear relation[16]

$$T_m = T_{m0} + B_T(\lambda_E - 1); \quad T_m = T, \lambda = \lambda_E \qquad (7)$$

The temperature of the experiment is the melting temperature at λ_E. The extrapolated temperature T_{m0} ($\lambda_E = 1$) is the melting temperature of pure NR in the isotropic state; the slope $B_T = dT_m/d\lambda$ is higher for F-NR ($B_T = 50$ °C) than for pure NR ($B_T = 30$ °C). This relation for pure NR is the well-known linear relation between the melting temperature and the draw ratio observed by various authors[11,15,52,53] using WAXS measurements

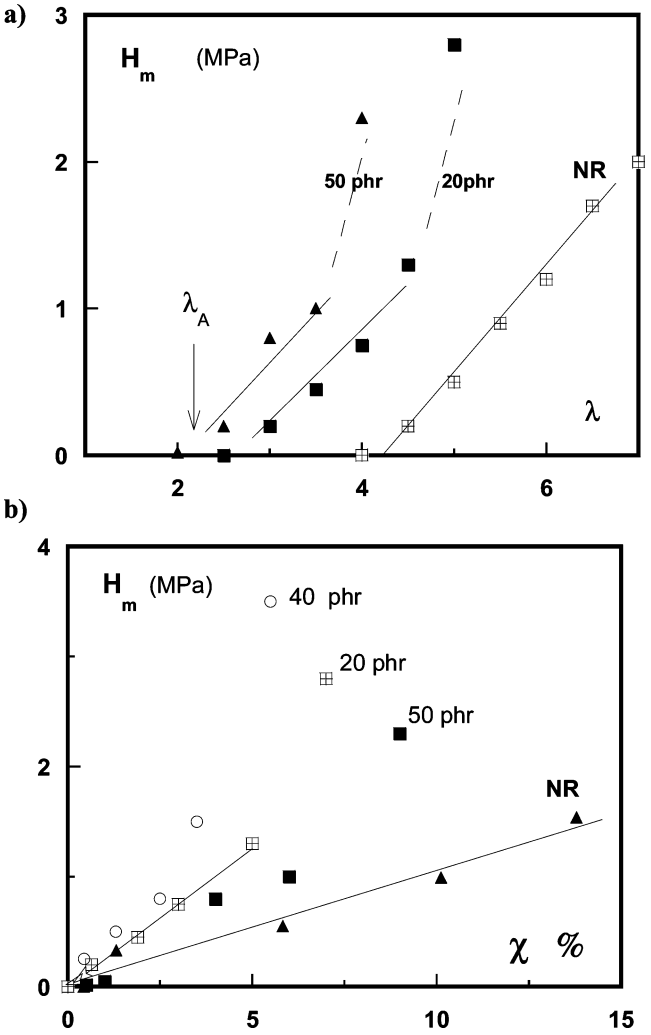

Figure 7. Mechanical hysteresis H_m of NR and F-NR as a function of the crystallinity χ measured at the maximum draw ratio ($\lambda = \lambda_C$) of the cycle at 22 °C (a) and as a function of the maximum draw ratio, $\lambda = \lambda_C$ (b). Lines are guides for the eyes.

and predicted by the Flory theory (and related theories, see the above references). B_T decreases with the filler content; this is due to the amplification of the strain in the F-NR samples. λ_E in filled samples is not the local draw ratio of the chains at the end of melting.

(2) $\Delta\lambda$ decreases with the filler content at any temperature. At any constant draw ratio Figure 6a gives the supercooling $T_m - T_c$. This difference between the melting and crystallization temperatures is of the order of 50 °C for pure NR and 20 °C for the 40 and 50 phr samples. This indicates clearly that the filler particles act as nucleation centers for the crystallization.

(b) Amplification Factor A_χ. The crystallinity curves of filled samples during stretching and recovery can be put into coincidence with the corresponding curves of the nonfilled samples by the orthogonal transformation $1 - \lambda_{NR} \Rightarrow A_\chi(1 - \lambda_{F-NR})$. As noted above for A_σ, this new amplification factor is different if the stretching or the recovery curve is concerned; also, it varies somewhat with the deformation. For example, the SA values A_χ of the 50 phr sample are 2 and 1.45 near λ_A and λ_E. It must be noted that melting is a thermodynamical transition, and there is no delay in melting; therefore, in the Flory relation, $T_m(\lambda)$, λ is the true strain (the local strain λ_l) at the temperature of experiment ($T_m = T$). In the following A_χ is determined from the experimental values λ_E obtained by WAXS measurements (Figures 3 and 4).

(c) Mechanical and Crystallinity Hysteresis. In Figure 7a,b we compare the mechanical hysteresis H_m of F-NR and NR samples as a function of the maximum draw ratio $\lambda = \lambda_C$ of the mechanical cycle and as a function of the maximum crystallinity, $\chi = \chi_m$, observed at λ_C. We have shown previously[15,52] that in pure natural and synthetic NR this hysteresis varies linearly with χ and λ_C. The same behavior is observed for F-NR samples. For all samples H_m extrapolates to zero for the critical draw ratio λ_A (Figure12 of ref 52 and Figure 6 of ref 15). The mechanical hysteresis ($\epsilon > 1$) is essentially due to the stress-induced crystallization (and melting) and not to the viscoelastic properties of the rubber matrix. The temperature of the experiments is about 90 °C above T_g; the (plateau) modulus would be independent of the time of measurement (several minutes). This conclusion obviously does not hold at shorter times. It is well-known that crystallizing and noncrystallizing filled rubbers show the Payne effect;[1,3] at low strain ($0.01 < \epsilon < 0.1$) and at higher frequency ($\omega > 1$ Hz) the maximum energy dissipated during a cycle is dependent on strain amplitude and filler concentration, and this last effect would be due to the rupture and reorganization of the aggregates and not to SIC.

(d) Variation of the Amplification Factors A_σ and A_χ with Filler Content. The amplification factor A_σ is deduced from the stress−strain curve in the stretching domain. The method is described in Figure 1b. During stretching A_σ presents weak but nonmonotone variations. At high deformation this factor has no straightforward meaning because it compares materials of different crystallinity. It is important to note that A_σ at low deformation, $1 < \lambda_{F-NR} < 1.8$, is constant and independent of the temperature. Above a critical draw ratio which corresponds to the onset of crystallization λ_A ($\lambda_A = 2$ for the 50 phr NR; see Figure 3c) the curve λ_{NR} (λ_{F-NR}) presents a jump. After this jump, during SIC and stress hardening the amplification factor decreases slowly with the draw ratio. In Figure 8 we have reported the strain amplification factor A_σ measured at low deformation, $\lambda < \lambda_A$, by the method of Figure 1b. By linear regression we obtain the following relation:

$$A_\sigma = 1 + 13.4C; \quad \lambda < \lambda_A \tag{8a}$$

The correlation factor of the fit is $R = 0.98$. The fit with the Guth and Gold relation (2) gives

$$A_\sigma = 1 + 6.9C + 38C^2; \quad \lambda < \lambda_A(\mathrm{GG}) \tag{8b}$$

the correlation factor being $R = 0.995$.

From the stress−strain curves of similar filled NR reported by Lee and Donovan[60] we deduce a similar relation. We must note that these amplification factors are much higher than those predicted by geometric considerations (eq 1c); this fact and the fact that A_σ is independent of T suggests that at low deformation the fillers act as cross-links (GNC). In this low deformation domain we can compare A_σ to the strain amplification factor A_χ deduced from the curves $T_m(\lambda_E)$. As λ_E for NR and F-NR varies linearly with T and converge to $T_{m0} = -20$ °C (eq 7), it is not necessary to use the method of Figure 1b. The amplification factor A_χ is the ratio of the slope B_T(NR)/B_T(F-NR). The values of A_χ for the three F-NR samples are given in Figure 8; linear regression leads to the relation

$$A_\chi = 1 + 3.4C; \quad \lambda_E < \lambda_A \tag{9}$$

As there is no delay in the melting, T_m in the two types of NR gives the real (local) extension of the chains via eq 7. Therefore,

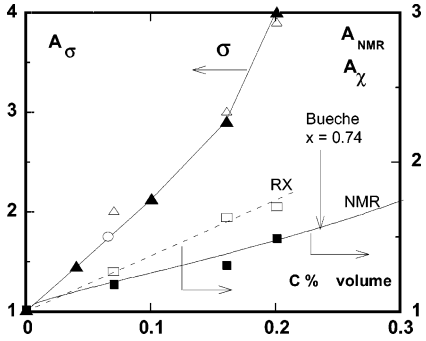

Figure 8. Strain amplification factors obtained respectively by mechanical (A_σ, triangle), NMR (A_{NMR}, filled squares), and WAXS (A_χ, empty squares) measurements as a function of the carbon black concentration. A_σ (empty triangles) is deduced from the stress−strain curves, Figure 1b, filled triangles data from Lee et al.[60] A_χ is deduced from the melting temperatures, eq 7. A_{NMR} is deduced from the splitting curves Figure 11b at low deformation in the stretching domain. Lines are guides for the eyes; the NMR results are fitted with the Bueche expression (see text).

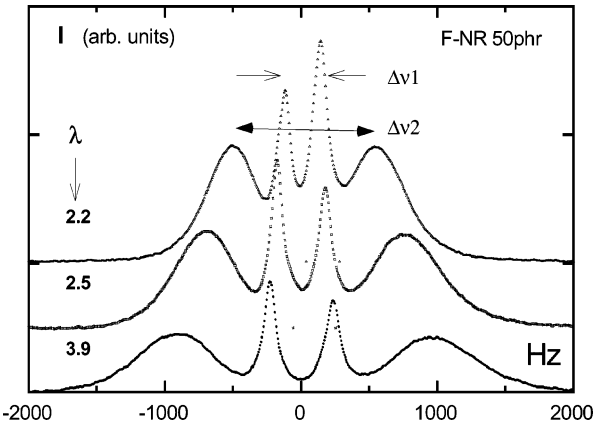

Figure 9. Quadrupolar NMR spectra of the F-NR 50 phr sample containing 1% of deuterated dodecane. Samples have been drawn at $\lambda = 2.2$, 2.5, and 3.9. The splitting of the two doublets due to the CD_3 and CD_2 bonds are indicated.

the strain amplification factor A_χ is the real strain amplification factor $A_\chi = A_\epsilon$, measured at λ_E. The direct measurement by NMR of the local extension λ_l of the chains in the filled samples will confirm this conclusion.

When the filled NR has crystallized, $\lambda > \lambda_A$, one can calculate the amplification factors A_χ and A_{Hm} from the crystallinity curves $\chi(\lambda)$ of Figure 3 and from the mechanical hysteresis $H_m(\lambda)$ of Figure 7b. The NR and F-NR curves can be superimposed by the transformation $1 - \lambda_{NR} \Rightarrow A(1 - \lambda_{F-NR})$ if A varies in an important way. For example, A_{Hm} varies from 3 to 1.8 and A_σ from 2.6 to 2.5 between $\lambda = 2$ and $\lambda = 3.5$ for the 50 phr sample. These factors compare NR materials which have been crystallized at different supercooling and then having different crystallinity; therefore, the respective roles of the crystallites and fillers cannot be separated easily.

4.2. Amorphous Chain Orientation: NMR Study. *4.2.1. NMR Spectra at Low Deformation.* Typical NMR spectra of F-NR 50 phr with 1% of deuterated dodecane ($n = 12$) drawn at various draw ratio are given in Figure 9. Similar spectra are observed for pure NR. There is no time evolution of the spectra, and this indicates that the high molecular weight solvent (boiling point 215 °C) is not expelled during the experiment. Also, the same spectra have been found for different probe concentrations (0.5−2%). The signal consists of two doublets of splitting $\Delta\nu_1$ and $\Delta\nu_2$; the smaller one is due to the CD_3 bonds and the other to the five different CD_2 groups along the alkane chain. The area of the peaks is proportional to the number of deuterium belonging to these groups ($I_{CD_2}/I_{CD_3} = 20/6 = 4.3$).

Quadrupolar splittings are given by the well-known relation for uniaxial deformation:

$$\Delta\nu = (3/2)\nu_q P_2(\cos\Omega)\langle P_2(\cos\theta(t))\rangle \qquad (10)$$

The brackets $\langle\ \rangle$ holds for a time average over motions faster than $1/\nu_q$. The angle between the magnetic field and the draw axis is $\Omega = 0°$. The quadrupolar frequency is of the order of $\nu_q = 175$ kHz for the C−D bonds. The angle θ in the second Legendre polynomials connects the experimental coordinate system with the direction of the C−D bonds; this angle fluctuates during the time t. In the fast motion regime, quadrupolar splitting $\Delta\nu_i$ of probes are proportional to the average of the chain orientation.[61,62]

The observed spectra are well resolved, with narrow lines; this indicates that we are indeed in the regime of fast diffusion. The time of the segmental motion is rapid compared to the quadrupolar characteristic time $t_q = 1/\nu_q \sim 10^{-5}$ s, the temperature of the experiments being 90 °C above the glass temperature of NR. In that condition the average $\langle P_2(\cos\theta(t))\rangle$ of the probes is proportional to the entropic elasticity term $(\lambda^2 - 1/\lambda)$ of the chains and inversely proportional to the effective molecular mass M_c^* between cross-links (eq 5a). The splitting writes

$$\Delta\nu = k(1/M_c^*)(\lambda^2 - 1/\lambda) = k_\nu(\lambda^2 - 1/\lambda) \qquad (11)$$

In pure NR the deformation is affine; the macroscopic draw ratio λ and the local one λ_l are equal. In filled samples λ must be replaced by λ_l. The constant k depends only on the local CD bond orientation in the alkane chain (on the stereochemical structure of the probe, i.e., on the location of the CD_2 and CD_3 group in the probe molecule). The variation of the slope $k_\nu = \Delta\nu/(\lambda^2 - 1/\lambda)$ with M_c^* has been observed in various network systems.[24−26,33,35,63,64] In nonfilled NR the dependence of k_ν on the cross-link density has been studied; by extrapolating k_ν to zero cross-link concentration ($1/M_c = 0$ in eq 5a) one deduces the molecular weight M_e of the chains between entanglements.

In Figure 10a the splitting $\Delta\nu_1$ due to CD_3 end groups is given as a function of $\lambda^2 - 1/\lambda$ for the four different samples at ambient temperature for small macroscopic deformation ($1 < \lambda < 1.6$). In this domain the rubber matrix has not crystallized, eq 11 is verified, and the slope $k_\nu = d\Delta\nu/d(\lambda - 1/\lambda^2) \sim 1/M_c^*$ increases with the CB content. One concludes that this effect is due to strain amplification, $\lambda_l Z > \lambda$, or/and to the increase of the effective cross-link density $d_{cl}^* \sim 1/M_c^*$ due to the formation of GNC. In pure NR this slope, as recalled above, increases with the cross-link density. In Figure 10b, the effects of cross-linking density and of filler content are compared. The slope k_ν of unfilled NR varies linearly with the mass m_s of sulfur. For the same mass of sulfur ($m_s = 1.2$ g phr) this slope varies also linearly with the filler content. We are tempted to conclude that the effect of the filler and sulfur cross-links present similar trends.

4.2.2. Deformation Cycles. In Figure 11a the splitting curve $\Delta\nu_1(\lambda^2 - 1/\lambda)$ is reported for high deformations ($1 < \lambda < 5$). We remark that two linear regimes are observed; the crossover between these regimes corresponds to the onset of crystallization at λ_A (arrows for the 50 phr and for the unfilled NR in the figure). In NR during stress-induced crystallization at $\lambda > \lambda_A$ ($\lambda_A \sim 4$) the splitting remains nearly constant up to $\lambda_C = 7$, which is the maximum draw ratio before rupture. This essential property is explained by the model of crystallization discussed in ref 53; during crystallization the remaining amorphous chains,

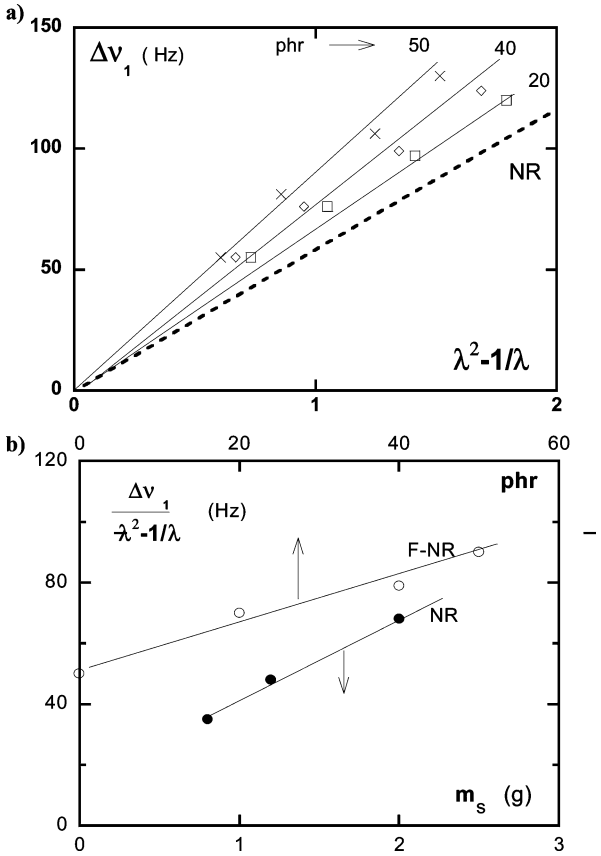

Figure 10. (a) NMR splitting $\Delta\nu_1$ of NR and F-NR samples as a function of the elasticity term $\lambda^2 - 1/\lambda$, at room temperature during stretching, λ is the macroscopic deformation. In this domain of low extension, $1 < \lambda < 1.3$, there is no stress-induced crystallization. Samples contain 2% deuterated dodecane. Lines are obtained by linear regression. (b) Comparison between the effects of density of cross-links (mass of sulfur m_s) in NR and concentration of carbon black (phr) in filled NR on the slope k_ν of the $\Delta\nu_1(\lambda^2 - 1/\lambda)$ curves in (a) at low deformation. The filled samples have 1.2 g of sulfur phr. NR data from ref 51.

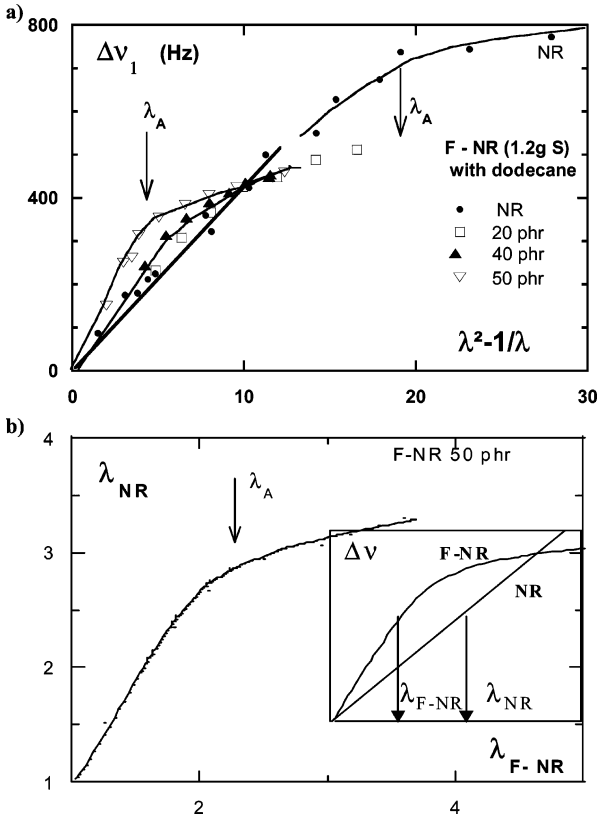

Figure 11. (a) NMR splitting $\Delta\nu_1$ of NR and F-NR samples as a function of the elasticity term $\lambda^2 - 1/\lambda$, at large extension, $1.16 < \lambda < 5$. The change in the slope in both types of rubbers during stretching (indicated by arrows for the 50 phr and pure NR) corresponds to the value of λ_A, the onset of stress-induced crystallization, obtained by mechanical and WAXS measurements. In NR crystallization begins at $\lambda_A = 4.2$; the splitting remains constant up to the rupture $\lambda \sim 7$. (b) Method for measuring the amplification factor A_{NMR}; see text and Figure 1b. In the inset, schematic view of the $\Delta\nu_1(\lambda)$ curves of NR and F-NR 50 phr of (a). The filled NR drawn at the macroscopic $\lambda = \lambda_{F-NR}$ has the chains locally drawn at $\lambda_l = \lambda_{NR}$. At low deformation (not crystallized samples) the strain amplification factor A_{NMR} at low deformation is the slope of the $\lambda_{NR}(\lambda_{F-NR})$ curve.

previously drawn at $\lambda > \lambda_A$, relax partially to $\lambda = \lambda_A$. In filled NR we remark a somewhat different behavior. Above λ_A the splitting is no longer constant but varies slowly and linearly with the entropy term $(\lambda^2 - 1/\lambda)$. All the curves $\Delta\nu_1(\lambda^2 - 1/\Lambda)$ pass through a same point at $\lambda = 3.6$. The properties reported here for F-NR samples at high extension are puzzling. Figure 11a demonstrates clearly that the splitting curves of NR and F-NR (stretching and recovery) cannot be superimposed by a simple and unique orthogonal transformation $1 - \lambda_{F-NR} \rightarrow A(1 - \lambda_{NR})$.

Here we were interested in the splitting $\Delta\nu_1$ due to the CD_3 groups; we stress that the same properties are observed if one plots $\Delta\nu_2$ as a function of $(\lambda^2 - 1/\lambda)$. As an example, we give in Figure 12a the splitting $\Delta\nu_1$ and $\Delta\nu_2$ of F-NR 50 phr as a function of the macroscopic deformation λ. The CD bonds of the CD_2 groups are obviously more oriented than those of the CD_3. During stretching (and recovery) the two splitting are proportional: $\Delta\nu_2(\lambda) = 3.7\Delta\nu_1(\lambda)$; the same relationship is found in nonfilled NR.[51] In the same figure we have reported the crystallinity curves during the deformation cycle (Figure 3d). We verify that the characteristic draw ratios λ_A and λ_E determined by the two techniques correspond. In Figure 12b, we compare the mechanical and NMR cycles obtained in equivalent conditions (at ambient temperature and same global deformation rate). It is noted that at λ_E, that is to say at the melting of the last crystallites, the NMR recovery and stretching curves $\Delta\nu_1(\lambda)$ merge. Also, we note that at the beginning of crystallization, at λ_A, the splitting curves $\Delta\nu(\lambda)$ present a change of slope (see Figures 11 and 12). In F-NR and in pure NR samples as soon as crystallization appears the remaining amorphous chains become less oriented than in the noncrystallized sample. The effect of drawing is less efficient on the orientation of the amorphous chains when SIC occurs. This is an effect suggested by Flory[8] but to our knowledge never verified (see for example Figure 12.6 of ref 5 and Figure 13 of ref 53).

In conclusion, by quadrupolar NMR in filled and unfilled NR (swollen with a low concentration of deuterated alkane) one determines with accuracy the critical draw ratio λ_A and λ_E for stress-induced crystallization and melting. At high deformation, in the hardening domain, the splitting is constant (NR) or weakly increasing with λ (F-NR). This again means that the reinforcement above the critical draw ratio λ_A in all samples is not due to the limited extensibility of the chains but to the formation of crystallites which act as GNC.

4.2.3. NMR Strain Amplification Factor A_{NMR}. In Figure 11b we apply the method of Figure 1b to calculate the amplification factor A_{NMR} in the low deformation domain, $\lambda < \lambda_A$. In the inset we reproduce the splitting curves $\Delta\nu_1(\lambda)$ of NR and F-NR (50 phr) as an example; the curves are smoothed, n values of $\Delta\nu$ are chosen arbitrarily, and the corresponding draw ratios

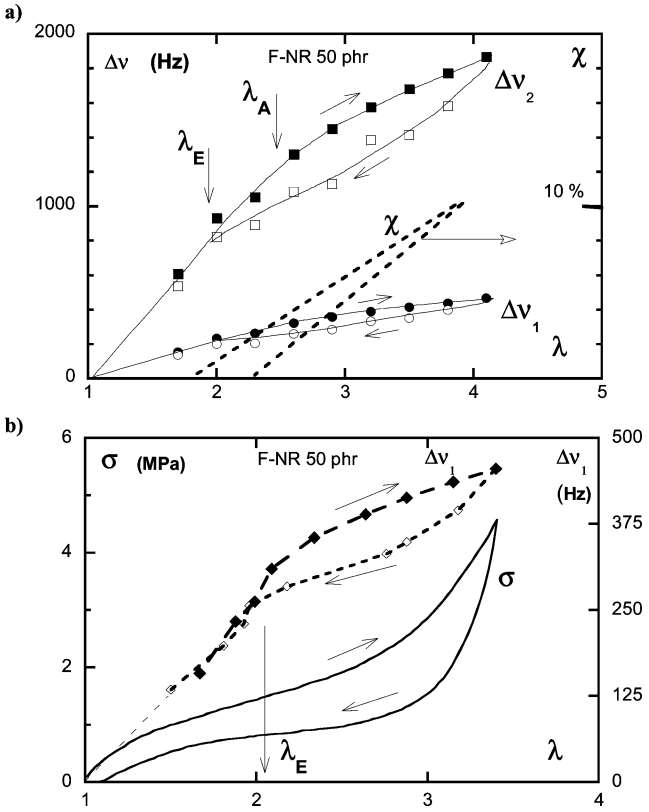

Figure 12. (a) NMR splitting $\Delta\nu_1$ and $\Delta\nu_2$ due to CD_3 and CD_2 groups of dodecane (1%) in F−NR 50 phr samples as a function of the macroscopic draw ratio λ. In dashed line the crystallinity curves; see Figure 3d. Lines are guides for the eyes. By WAXS and NMR one measures the same critical draw ratios λ_A and λ_E. (b) Same sample. Comparison between mechanical (σ) and NMR ($\Delta\nu_1$) cycles. The critical draw ratios λ_A (change of slope of the NMR stretching curve) and λ_E (merging of the stretching and recovery NMR curves) correspond to the values (crystallization and melting) observed by WAXS.

λ_{NR} and λ_{F-NR} are recorded. The curve $\lambda_{NR}(\lambda_{F-NR})$ gives the variation of the local draw ratio $\lambda_l = \lambda_{NR}$ as a function of the macroscopic draw ratio $\lambda = \lambda_{F-NR}$ of the filled sample. The amplification factor

$$A_{NMR} = \frac{\lambda_{NR} - 1}{\lambda_{F-NR} - 1} = \frac{\lambda_l - 1}{\lambda - 1} \qquad (12a)$$

is the true strain amplification factor. In the three filled samples, the slope of the curve $\lambda_{NR}(\lambda_{F-NR})$ is constant at low macroscopic deformation up to the critical draw ratio λ_A at the onset of crystallization. The values of A_{NMR} are compared to the other strain amplification factors in Figure 8. By linear regression one obtains

$$A_{NMR} = 1 + 2.5C; \quad \lambda < \lambda_A \qquad (12b)$$

When the filled NR does not crystallize, $\lambda < \lambda_A$, we conclude that:

(a) The strain amplification factors A_χ and A_{NMR} (eqs 7 and 12) are of the same order, the CB concentration dependence is similar to that predicted by Bueche (eq 1c), and the fit with eq 1b gives the exponent $x = 0.55$ (A_{NMR}) and 0.73 (A_χ) with a correlation factor $R = 0.99$. These exponents must be compared to the Bueche exponent $x = 0.33$ for an ideal three-dimensional arrangement of monodispersed rigid spheres in a rubber matrix and to $x = 1$ for a one-dimensional arrangement of soft and rigid lamellae.

(b) A_{NMR} is very different from the mechanical amplification factor A_σ deduced from this work (eq 8) and from the work of Lee and Donovan.[60] The experimental relation $(A_\sigma - 1)/(A_{NMR} - 1) \sim 5$ (Figure 8) indicates that reinforcement for $\lambda < \lambda_A$ is not due solely to the more important local extension of the amorphous chains in the filled NR but also to an additional cross-linking effect: the increase of the density of effective cross-links due to the constraints added by the fillers on the chains. As recalled in the Introduction, such a role of the CB particles was suggested by Flory a long time ago.

Berriot et al.[59] analyzing the magnetization relaxation time of isotropic polyacrylate matrix filled with silica particles concluded that "topological constraints localized at the interfaces have the same effect on the magnetization relaxation as the cross-links (and entanglements) homogeneously distributed in the matrix". In our strained filled rubbers these constraints which increase with the filler content produce a greater effect on the modulus ($A_\sigma = 1 + 13C$) than on the local strain ($A_{NMR} = 1 + 2.5C$). We postulate then that the amplification factor A_σ deduced from the stress−strain curves is due to both effects: the amplification of the strain and the increase of modulus. In other words, the $\sigma(\lambda)$ curve of the filled rubber is deduced from that of the unfilled rubber by two successive orthogonal transformations of ratio $(A_\epsilon)^{-1}$ and E_0/E. We assume that in filled rubber the effective cross-link density increases linearly with the volume fraction of filler, $d^*_{cl}/d_{cl} = E/E_0 = 1 + yC$. Taking into account eq 12b, we obtain

$$A_\sigma = (d^*_{cl}/d_{cl})A_\epsilon = (1 + yC)(1 + 2.5C) \qquad (13)$$

This is the Guth and Gold (GG) relation, eqs 2 and 8b, with $a = y + 2.5$ and $b = 2.5y$; the fit with the data of Figure 8 gives $y = 7.6$, and the correlation coefficient is $R = 0.99$. By this fitting procedure, we obtain the GG relation: $A_\sigma = 1 + 10C + 20C^2$. The accuracy of the measurements does not permit to conclude which form of the GG relation (eq 8b or eq 13) is more appropriate.

Typically, for $C = 0.15$, $d^*_{cl}/d_{cl} \sim 2$. The effect of constraints created locally by the particles is equivalent to an increase of density of cross-links $d^*_{cl} - d_{cl} \sim d_{cl}$ homogeneously dispersed in the matrix.

4.2.4. Homogeneity of the Deformations. In filled rubbers the structure and the morphology observed by electron microscopy and AFM are not uniform; particles are aggregated, and the size of these agglomerates and the distance between aggregates are not uniform. Also in some circumstances we have found that in pure rubber during recovery the material contains two phases in equilibrium (inverse yielding effect[53]). One wonders if the local deformation and then the local stress are spatially nonhomogeneous in these materials (in particular during stretching). It is important to give an estimate of the length scale over which the splitting is averaged.

Unnikrishnan et al.[65] have measured the diffusion coefficient D of four *n*-alkanes (hexane to nonane) in natural rubber vulcanized via different ways. In NR vulcanized by sulfur ($M_c \sim 15\,500$, $N_c \sim 229$) they observed a decrease of D with the length of the probes. Linear extrapolation of their results to dodecane leads to $D \sim 10^{-5}$ cm^2/s; in our systems the deuterated probes diffuse in the rubber matrix over a length, l_q, relative to $(Dt_q)^{0.5}$, which is of the order of 100 nm for the quadrupolar characteristic time ($t_q = 1/\nu_q \sim 10^{-5}$ s). Obviously this length is reduced in F-NR by the solid particles (carbon black, NR, and stearic acid crystallites); for a crystallinity of 10% the mean distance between crystallites is about 20 nm, and in the 40 phr

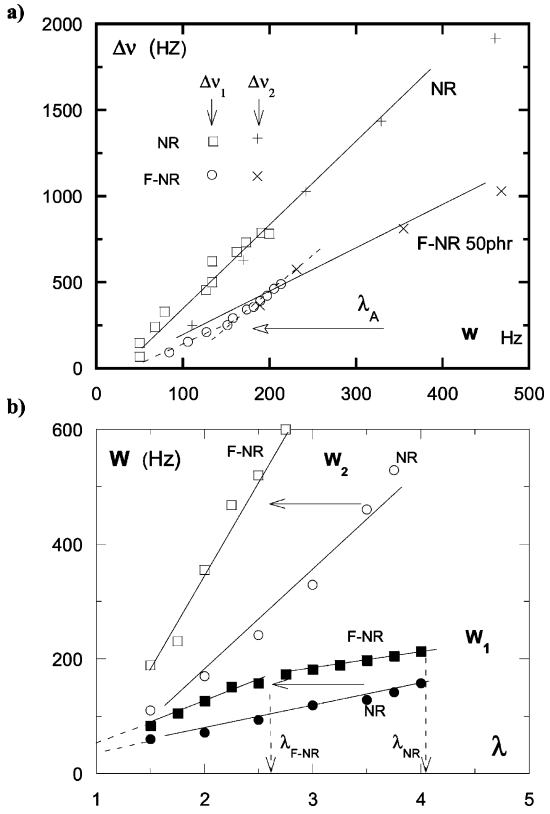

Figure 13. (a) Correlation between the splitting $\Delta\nu_i$ and the width W_i of the NMR peak doublets CD_3 (square, NR; circle, F-NR) and CD_2 (+, NR; ×, F-NR). Lines are guide for the eyes. (b) Comparison of the width W_i of the two doublets peaks CD_3 and CD_2 of NR and F-NR (50 phr) as a function of the macroscopic deformation. At low deformation, $\lambda < \lambda_A$, the two curves $W_1(\lambda)$ and $W_2(\lambda)$ of the NR and F-NR samples can be superimposed by the transformation $(\lambda_{F-NR} - 1) \rightarrow A_W(\lambda_{NR} - 1)$. The amplification factor A_W is of the order of 1.5−1.7.

isotropic and stretched samples the mean distance between CB particles and aggregates is 100−600 nm (see for example ref 21). In conclusion, the length scale over which the splitting is averaged is of the order of 10−100 nm; this is smaller than the mean distances between carbon black aggregates and NR crystallites. It would be important in the future to know if NR (filled and nonfilled) presents heterogeneities of this size and to understand the origin of such heterogeneities.

The line width of the NMR peaks depends in a complex manner on the static and dynamic heterogeneities.[66] We have found that the width W and the splitting $\Delta\nu$ of these oriented materials do not depend on the molecular weight of the probe (eicosane, dodecane, decane, nonane) and its concentration (<4%). This behavior indicates that $\Delta\nu$ and W are not dependent on the diffusion coefficient of these types of probes. A different result has been reported by Simon;[24] in SBR networks swollen with deuterated benzene $\Delta\nu$ and W do depend on the concentration φ of the NMR probes. We have remarked that the width W_i and the splitting $\Delta\nu_i$ increase with the deformation (see for example Figure 9), and we have then plotted in Figure 13a $\Delta\nu_1$ vs W_1 for the unfilled and filled (50 phr) samples; similar plots are obtained for the other samples. For a same splitting, that is to say for a same local deformation (same $\Delta\nu$), the line width of the CD_3 peaks of the filled sample is 1.6 times broader than that of the unfilled one. The same conclusion is reached if we plot $\Delta\nu_2$ vs W_2 (in the figure, symbols + and ×).

The simultaneous increase of W and $\Delta\nu$ with rising deformation was observed by Menge et al.[64] in unfilled polybutadiene with deuterated dangling and cross-linked chains and by Valic et al.[67] in polybutadiene networks swollen with deuterated chains.

As W could be an indication of the heterogeneity of the rubber, we have compared in Figure 13b the variation of the line widths W_1 and W_2 with the macroscopic draw ratio of the filled (50 phr) and unfilled samples. From this figure we conclude that:

(a) The widths of the CD_2 and CD_3 peaks of all materials vary linearly with the deformation; extrapolation to $\lambda = 1$ leads to the observed value ($W \sim 50$ Hz) of the isotropic sample.

(b) In the low deformation regime, $\lambda < \lambda_A$, the width $W_i(\lambda)$ of the F-NR sample can be superimposed (arrows in the figure) with that of the NR sample by the transformation $(\lambda_{F-NR} - 1) \rightarrow A_W(\lambda_{NR} - 1)$. The amplification factor $A_W \sim 1.6$ is very near the value deduced from the splitting, $A_{NMR} \sim 1.5$ (Figure 8).

(c) In the high deformation regime $\lambda > \lambda_A = 2.2$ the width of the F-NR sample continue to increase with λ, but slower. The splitting $\Delta\nu$ and the width W present similar variations; the crossover between the two regimes correspond to the critical draw ratio, λ_A, for the onset of the stress-induced crystallization.

The striking feature of these results is the similar line broadening observed in filled and nonfilled rubbers: the samples being drawn at different draw ratios but having the same splitting (that is to say the same local extension λ_l). Since the line width is always proportional to the splitting (and the fact that the slope $\Delta\nu/W$ does not depend on the mass and concentration of the deuterated probes), it is likely that the broadening is homogeneous. This conclusion should be verified by other NMR techniques.[68−70] Also, it would be interesting to compare the line shapes of filled NR-containing deuterated probes and cross-linked PI chains, although the origins are different.[35,61,62]

5. Conclusion

By WAXS and quadrupolar NMR we have shown that the stress-induced crystallization and melting in filled rubber can be followed very accurately. The critical drawing ratios for appearance and disappearance of the NR crystallization correspond to the critical values, λ_A and λ_E, deduced from the stress−strain curves. The main interest of the NMR technique is to give a mean value, with a high accuracy, of the local extension of the amorphous chains during the processes of crystallization and melting, during stretching and recovery.

From the variation of the property X with the strain (in stretching experiments) we have defined the strain amplification factors A_X (X: stress, crystallinity, mechanical hysteresis, NMR splitting, and line broadening). These factors vary with deformation as soon as crystallization (or melting) begins during stretching (or recovery). The NMR amplification factor A_{NMR} gives the true strain amplification in all domain of deformation, the sample being partially crystallized or not, during stretching or during recovery. From the melting of NR crystallites (observed by WAXS) we deduce the deformation of the amorphous chains and then calculate the amplification factor A_χ. Amplification factors A_{NMR} (and A_W) and A_χ are of the same order of magnitude and vary with the filler concentration as predicted by eq 1b with the exponent $x = 0.75$; the arrangement of particles (aggregates) in the rubber soft matrix cannot be considered as a three-dimensional, $x = 1/3$, or a one-dimensional regular arrangement, $x = 1$.

At low deformation, before stress-induced crystallization, the strain amplification factors A_σ and A_{NMR} of F-NR samples are very different. The relation $A_\sigma \sim 2.5A_{NMR}$ (Figure 8) indicates clearly that the reinforcement in filled rubber at low deformation

is due to both effects: the overstrain of the chains and the increase of the cross-link density due to the filler. These effects are coupled and of the same magnitude. The density of constraints d_{cl}^*, added by the fillers (eq 13), is comparable to the density d_{cl} of sulfur cross-links and entanglements for $C > 0.2$. We think that the static properties of vulcanized rubbers (stress, modulus, measured at very low rate) cannot be explain by the comparison with dynamic properties of the unvulcanized rubber (viscosity); according to our model the quadratic term of the GG empirical relation is due to the coupling between these two effects (eq 13) and not to the hydrodynamic interactions between particles, as is generally accepted. Finally, at low deformation we point out that our NMR results on F-NR and the SANS results of Westermann et al.[38] on composite model system (PS−PI−PS) confirm the model for the strain enhancement in reinforced networks. By SANS on silica-filled rubbers Botti et al.[42] found quite different results attributed to the breaking-up processes in the filler systems. We think that at low deformation the aggregates in F-NR do not break and/or do not deform.

During stress hardening, $\lambda > \lambda_A$, crystallinity increases linearly with draw ratio, and during recovery the reverse effect is observed. The main difference between filled and nonfilled samples is the supercooling effect: the difference $\lambda_A - \lambda_E$ decreases with the increase of CB concentration. CB particles act as nucleation centers of the NR crystallites. This effect would be due to the nonuniform extension of the chains in such heterogeneous materials. Around a particle, as at a crack tip, the chains are overstrained and crystallization is accelerated;[14,60] this SIC process relaxes the remaining amorphous chains. This primarily crystallization would then carry on far from the particles. The crystallization process can be considered as a healing process which put off the rupture of the chains previously overstressed. NR and F-NR in the hardening domain are equivalent to new materials, cross-linked by the small crystallites in addition with the sulfur bridges and with the giant network cross-links constituted by the fillers.

During hardening the extension of the remaining amorphous chains in filled and unfilled NR is no longer affine. The local draw ratio in F-NR measured by NMR increases weakly with λ, whereas the crystallinity varies linearly from 0 at $\lambda_A = 2.5$ to 10% at $\lambda_C = 4$. The increase of the stress $\sigma(\lambda_C) \sim 5\sigma(\lambda_A)$ in this domain cannot be explained by the corresponding increase of local draw ratio $\lambda_C(\text{local})/\lambda_A(\text{local}) = \Delta\nu_1(\lambda_C)/\Delta\nu_1(\lambda_A) \sim 1.5$. As suggested by Flory and discussed in refs 51 and 52 in this domain the NR crystallites should be considered as additional cross-links in the rubber network. As each crystallites formed during stretching has the same dimensions, the density of additional cross-links has then the form $d_{cryst} \sim c \sim (l - l_A)$; above λ_A the splitting and then the local extension of the chains increases linearly with the macroscopic draw ratio $\lambda_l \sim \lambda$. The stress given by the classical elasticity theory $\sigma \sim d_{cl}^*(\lambda_l - \lambda_l^{-2})$ has then the scaling form $\sigma \sim d_{cryst}(\lambda_l - \lambda_l^{-2}) \sim \lambda(\lambda - \lambda_A)$. The effectiveness of the crystallites as new cross-links would depend on the macroscopic deformation. At the beginning of crystallization the crystallites are formed of folded chains; at the end of the process many chains are connecting the crystallites of the super network.

Finally as for pure NR, we have shown that the mechanical hysteresis is due mainly to the crystallization and melting processes. It is well-known that this first-order transitions lead to important hysteresis (due to the supercooling).

Acknowledgment. We thank Dr. P. Johnson, Dr. J. M. Favrot, and Dr. K. Haug from Michelin Co. and Dr. B. Deloche and Dr. P. Sotta for stimulating discussions and remarks about this work.

References and Notes

(1) Kraus, G. In *Reinforcement of Elastomers*; Interscience Pub.: New York, 1965; p 64.
(2) Dannenberg, M.; Brennan, J. *J. Rubber Chem. Technol.* **1965**, *39*, 597.
(3) Kraus, G. *Adv. Polym. Sci.* **1971**, *8*, 155.
(4) Donnet, J. B.; Voet, A. In *Physics, Chemistry and Elastomer Reinforcement*; Marcel Dekker: New York, 1976.
(5) Mark, J. E.; Erman, B. In *Rubber Elasticity a Molecular Primer*; Wiley-Interscience: NewYork, 1988.
(6) Edwards, D. C. *J. Mater. Sci.* **1990**, *25*, 4175.
(7) Rajeev, R. S. *Rubber Chem. Technol.* **2002**, *75*, 475.
(8) Flory, P. J. *J. Chem. Phys.* **1947**, *15*, 397.
(9) Gent, A. N. In *Engineering with Rubber*; Oxford University Press: New York, 1992.
(10) Gent, A. N. *Rubber Chem. Technol.* **1996**, *69*, 834.
(11) Gent, A. N. In *Science and Technology of Rubber*; Mark, J. E., Erman, B.. Eds.; Academic Press: New York, 1994.
(12) Thomas, A. G.; Whittle, J. M. *Rubber Chem. Technol.* **1970**, *43*, 222.
(13) Lee, D. J.; Donovan, J. A. *Rubber Chem. Technol.* **1987**, *60*, 910.
(14) Trabelsi, S.; Albouy, P. A.; Rault, J. *Macromolecules* **2002**, *35*, 10054.
(15) Trabelsi, S.; Albouy, P. A.; Rault, J. *Rubber Chem. Technol.* **2004**, *77*, 303.
(16) Trabelsi, S.; Albouy, P. A.; Rault, J. *Macromolecules* **2003**, *36*, 9093.
(17) Flory, P. J. In *Principles of Polymer Chemistry*; Cornell University Press: Ithaca, NY, 1953.
(18) Kraus, G. *Angew. Makromol. Chem.* **1977**, *60*/*61*, 215.
(19) Dannenberg, E. M. *Prog. Rubber Plast. Technol.* **1985**, *1*, 13.
(20) Göritz, D. *Angew. Makromol. Chem.* **1992**, *202*/*203*, 309.
(21) Reichert, W. F.; Göritz, D.; Duschl, E. J. *Polymer* **1993**, *34*, 1216.
(22) Reichert, W. F.; Hopfenmuller, M. K.; Göritz, D. *J. Mater. Sci.* **1987**, *22*, 3470.
(23) Bokobza, L. *Macromol. Mater. Eng.* **2004**, *289*, 607.
(24) Deloche, B.; Samulski, E. T. *Macromolecules* **1981**, *14*, 575.
(25) Dubault, A.; Deloche, B.; Hertz, J. *Polymer* **1984**, *25*, 1405.
(26) Dubault, A.; Deloche, B.; Hertz, J. *Macromolecules* **1987**, *20*, 2096.
(27) Gronski, W.; Stadler, R.; Jacobi, M. M. *Macromolecules* **1988**, *17*, 741.
(28) Baumann, K.; Gronski, W. *Kautschuk Gummi Kunst.* **1989**, *42*, 383.
(29) Simon, G. *Polym. Bull. (Berlin)* **1991**, *25*, 365.
(30) Simon, G.; Schneider, H. *Makromol. Chem., Makromol. Symp.* **1991**, *C233*, 52.
(31) Litvinov, V. M.; Spiess, H. W. *Makromol. Chem.* **1992**, *193*, 1181.
(32) Waldhieser, K. M.; Cohen, C.; Duncan, T. M. *Macromolecules* **1997**, *30*, 1044.
(33) Deloche, B.; Sotta, P. In *Spectroscopy of Rubbers and Rubbery Materials*; Litvinov, V. M., De, P. P., Eds.; Rapra Technology Ltd.: UK, 2002.
(34) Litvinov, V. M.; Steeman, P. A. M. *Macromolecules* **1999**, *32*, 8476.
(35) Ries, M. E.; Brereton, M. G.; Klein, P. G.; Ward, I. M.; Ekanayake, P.; Menge, H.; Schneider, H. *Macromolecules* **1999**, *32*, 4961.
(36) Ekanayake, P.; Menge, H.; Schneider, H.; Ries, M. E.; Brereton, M. G.; Klein, P. G. *Macromolecules* **2000**, *33*, 1807.
(37) Westermann, S.; Kreitschmann, M.; Pyckhout-Hintzen, W.; Richter, D.; Straube, E. *Physica* **1997**, *B234*, 306.
(38) Westermann, S.; Kreitschmann, M.; Pyckhout-Hintzen, W.; Richter, D.; Straube, E.; Farago, B.; Goericgk, G. *Macromolecules* **1999**, *32*, 5793.
(39) Botti, A.; Pyckhout-Hintzen, W.; Richter, D.; Straube, E.; Urban, V.; Kohlbrecher, J. *Physica* **2000**, *B276*, 371.
(40) Bueche, A. M. *J. Appl. Phys.* **1952**, *23*, 154.
(41) (a) Bueche, F. *J. Appl. Polym. Sci.*. **1954**, *14*, 355. (b) Bueche, F. *J. Appl. Polym. Sci.* **1961**, *5*, 271.
(42) Botti, A.; Pyckhout-Hintzen, W.; Richter, D.; Urban, V.; Straube, E. *J. Chem. Phys.* **2006**, *124*, 17908.
(43) (a) Guth, E.; Gold, O. *Phys. Rev.* **1938**, *53*, 322. (b) Guth, E.; Gold, O. *J. Appl. Phys.* **1945**, *16*, 20.
(44) Mullin, L.; Tobin, N. R *J. Appl. Polym. Sci.*. **1965**, *9*, 2993.
(45) Rajeev, R. S.; De, S. K. *Rubber Chem. Technol.* **2002**, *75*, 475.
(46) Castaing, J. C.; Allain, C.; Auroy, P.; Auvray, L.; Pouchelon, A. *Europhys. Lett.* **1996**, *36*, 153.
(47) Elias, H. G. In *Macromolecules Structure and Properties*; Plenum Press: New York, 1977.
(48) Mitchell, G. R. *Polymer* **1984**, *25*, 1562.
(49) Samulski, E. T. *Polymer* **1985**, *26*, 177.
(50) Cohen-Addad, J. P. *J. Chem. Phys.* **1974**, *60*, 2440.
(51) Marchal, J. Ph.D. Thesis, University Paris-Sud, France, 2006.
(52) Trabelsi, S.; Albouy, P. A.; Rault, J. *Macromolecules* **2003**, *36*, 7624.
(53) Albouy, P. A.; Marchal, J.; Rault, J. *Eur. Phys. J. E* **2005**, *17*, 247.

CDV

(54) (a) Toki, S.; Fujimaki, T.; Okuyama, M. *Polymer* **2000**, *41*, 5423. (b) Toki, S.; Sics, I.; Ran, S.; Liu, L.; Hsiao, B. S.; Murakami, S.; Senoo, K.; Kohjiya, S. *Macromolecules* **2002**, *35*, 6573.
(55) Toki, S.; Sics, I.; Ran, S.; Liu, L.; Hsiao, B. S.; Murakami, S.; Tosaka, M.; Kohjiya, S.; Poompradub, S.; Ikeda, Y.; Tsou, A. H. *Rubber Chem. Technol.* **2004**, *77*, 317.
(56) Miyamoto, Y.; Yamao, H.; Sekimoto, K. *Macromolecules* **2003**, *36*, 646.
(57) Simon, G.; Baumann, K.; Gronski, W. *Macromolecules* **1992**, *25*, 3624.
(58) Maier, P.; Göritz, D. *Kautsch. Gum. Kunst.* **1996**, *49*, 18.
(59) Berriot, J.; Martin, F.; Montes, H.; Monnerie, L.; Sotta, P. *Polymer* **2003**, *44*, 1437.
(60) Lee, D. J.; Donovan, J. A. *Rubber Chem. Technol.* **1987**, *60*, 15.
(61) Sotta, P.; Deloche, B. *Macromolecules* **1990**, *23*, 1999.
(62) Sotta, P. *Macromolecules* **1998**, *31*, 3872.
(63) Waldhieser, K. M.; Cohen, C.; Duncan, T. M. *Macromolecules* **1997**, *30*, 1044.
(64) Menge, H.; Hotopf, S.; Schneider, H. *Polymer* **2000**, *41*, 4189.
(65) Unnikrishnan, G.; Thomas, S. *J. Polym. Sci., Part B: Polym. Phys.* **1998**, *35*, 725.
(66) Poon, C. D.; Samulski, E. T. *J. Non-Cryst. Solids* **1991**, *131*, 509.
(67) Valic, S.; Judeinstein, P.; Deloche, B. *Polymer* **2003**, *44*, 5267.
(68) Zeghal, M.; Auroy, P.; Deloche, B. *Phys. Rev. Lett.* **1995**, *75*, 2140.
(69) Zeghal, M.; Deloche, B.; Albouy, P. A.; Auroy, P. *Phys. Rev. E* **1997**, *56*, 5603.
(70) Meerwall, E.; Fergusson, R. D. *J. Polym. Sci., Phys.* **1981**, *19B*, 77.

MA0608424